# **Enhancing Cost Efficiency in Active Learning with Candidate Set Query**

Yeho Gwon \*1 Sehyun Hwang \*1 Hoyoung Kim 1 Jungseul Ok 1 Suha Kwak 1

https://yehogwon.github.io/csq

## **Abstract**

This paper introduces a cost-efficient active learning (AL) framework for classification, featuring a novel query design called candidate set query. Unlike traditional AL queries requiring the oracle to examine all possible classes, our method narrows down the set of candidate classes likely to include the ground-truth class, significantly reducing the search space and labeling cost. Moreover, we leverage conformal prediction to dynamically generate small yet reliable candidate sets, adapting to model enhancement over successive AL rounds. To this end, we introduce an acquisition function designed to prioritize data points that offer high information gain at lower cost. Empirical evaluations on CIFAR-10, CIFAR-100, and ImageNet64x64 demonstrate the effectiveness and scalability of our framework. Notably, it reduces labeling cost by 42% on ImageNet64x64.

## 1 Introduction

Deep neural networks owe much of their success to large-scale annotated datasets (Deng et al., 2009b; Kirillov et al., 2023; OpenAI, 2023; Radford et al., 2021). Scaling datasets is crucial for improving both of their performance (Hestness et al., 2017; Zhai et al., 2022) and robustness (Fang et al., 2022). However, the resources demanded for manual annotation pose a significant bottleneck, particularly in fields requiring expert input like medical data. In response to these challenges, cost-efficient methods for dataset collection, such as semi-automatic labeling (Kim et al., 2024; Qu et al., 2024; Wang et al., 2024), synthetic data generation (Liu et al., 2019; Tran et al., 2019), and active learning (AL) (Ash et al., 2020; Kirsch et al., 2019; Sener & Savarese, 2018; Settles, 2009; Sinha et al., 2019; Wang & Ye, 2015) have been studied.

Preprint.

This paper investigates AL for classification, where a training algorithm selects informative samples from the data pool and queries annotators for their class labels within a limited budget. We focus on improving the design of annotation queries, emphasizing their critical role. To be specific, we consider image classification of L classes. In the conventional design of query, an annotator is asked to choose a class in the list of L classes. Here, the effort needed to review the entire class list and identify the correct class increases as the list size L increases; according to an information-theoretic analysis (Hu et al., 2020), the cost of choosing among L options is  $\log_2 L$ . To address this issue of growing annotation cost, recent studies (Hu et al., 2020; Kim et al., 2024) employ a 1-bit query design asking annotators to check if the top-1 model prediction is correct. While this simplifies and speeds up annotation, it produces weak supervision incompatible with standard classification loss functions, necessitating specialized losses and algorithms like contrastive loss and semi-supervised learning techniques.

We propose *candidate set query* (CSQ), a novel AL query design that remains cost-efficient with increasing classes and integrates seamlessly with existing loss functions. CSQ presents the annotator with an image and a narrowed set of candidate classes, which is likely to include the ground-truth class. If the ground-truth class is within these candidates, the annotator selects from this smaller group; otherwise, they select from the remaining classes. This query approach can reduce labeling costs by reducing the search space required for annotation, which is particularly effective in scenarios with a wide range of classes where the search space for the annotator could be extensive. Figure 1(*left*) compares CSQ with the conventional query in AL for classification to show its efficiency.

In the CSQ framework, the design of the candidate set is crucial for its effectiveness. Too many candidates unnecessarily increase the labeling costs. On the other hand, too few candidates are likely to omit the ground-truth class, requiring an additional query to identify the ground-truth class among the remaining classes, which is more expensive than the conventional query. To enhance the effectiveness of the CSQ framework, we propose to construct can

<sup>\*</sup>Equal contribution <sup>1</sup>Pohang University of Science and Technology (POSTECH), South Korea. Correspondence to: Suha Kwak <suha.kwak@postech.ac.kr>.

didate sets guided by prediction uncertainty from a trained model using conformal prediction (Shafer & Vovk, 2008; Angelopoulos et al., 2023). Conformal prediction aims at constructing a set of predictions including the true class, where each set is properly sized based on the certainty of the model about the input. This strategy enables flexible adjustment of the candidate set for each sample, expanding it for an uncertain sample to include the true label and shrinking it for more certain one to reduce the labeling cost. Furthermore, we optimize the level of certainty in conformal prediction to minimize the labeling cost for each round. Therefore, this candidate set construction adapts to the increasing accuracy of the model over successive AL rounds, refining the candidate set as the model improves.

Last but not least, we propose a new acquisition function designed to maximize the cost efficiency of CSQ. Conventional acquisition functions in AL are designed to favor samples with high estimated information gain, assuming uniform annotation costs across all samples. On the other hand, in CSQ, the labeling cost for each sample varies according to the size of its candidate set. Thus, we propose an acquisition function that evaluates samples based on the ratio of estimated information gain to labeling cost. Specifically, we combine the conventional acquisition function score, which indicates the estimated information gain, with the estimated cost derived from the candidate set, favoring samples that maximize information gain per unit cost. This cost-efficient acquisition function can incorporate with any sample-wise acquisition score, ensuring the selection of both informative and cost-efficient samples.

The proposed method achieved state-of-the-art performance on CIFAR-10 (Krizhevsky et al., 2009), CIFAR-100 (Krizhevsky et al., 2009), and ImageNet64x64 (Chrabaszcz et al., 2017). We verify the effectiveness and robustness of CSQ through extensive experiments with varying datasets, acquisition functions, and budgets. Notably, CSQ achieves the same performance as the conventional query on ImageNet64x64 at only 42% of the cost, showing its scalability. Our ablation studies demonstrate that both our candidate set construction and sampling strategy contribute to the performance. Furthermore, the necessity of CSQ is demonstrated by a user study involving 40 participants. In short, the main contribution of this paper is four-fold:

- We propose a novel query design for active learning, where the annotator is presented with an image and a narrowed set of candidate classes that are likely to include the ground-truth class. This approach, termed CSQ, significantly reduces labeling cost by minimizing the search space the annotator needs to explore.
- To maximize the advantage of CSQ, we propose to

- utilize conformal prediction to dynamically generate small yet reliable candidate sets optimized to reduce labeling costs, adapting to the evolving model throughout successive AL rounds.
- We propose a new acquisition function that prioritizes a data point expected to have high information gain relative to its labeling cost, enhancing cost efficiency.
- The proposed framework achieved state-of-the-art performance on diverse image classification datasets, CIFAR-10, CIFAR-100, and ImageNet64x64, showing its effectiveness and generalizability.

### 2 Related Work

Acquisition functions in AL. The key to AL is to select and annotate the most informative samples (Settles, 2009; Dasgupta, 2011; Hanneke et al., 2014). To assess informativeness, various acquisition functions have been proposed, considering either the uncertainty of model predictions (Asghar et al., 2017; He et al., 2019; Ostapuk et al., 2019; Fuchsgruber et al., 2024; Kim et al., 2024; Cho et al., 2024; Kim et al., 2023), diversity in feature space (Sener & Savarese, 2018; Sinha et al., 2019; Yehuda et al., 2022), or both (Ash et al., 2020; Hwang et al., 2022; Wang & Ye, 2015; Wang et al., 2019; Hacohen et al., 2022; Hacohen & Weinshall, 2023a;b). Disagreement-based AL and its variants are supported by rigorous theoretical learning guarantees (Hanneke et al., 2014; Krishnamurthy et al., 2019). However, these methods assume uniform sample costs and select based solely on the amount of information. We emphasize that the labeling cost required for each sample varies and prioritize samples offering the best informationto-cost ratio.

Efficient query design. Designing efficient annotation queries reduces the annotation costs of crafting datasets. In AL, diverse types of queries have been investigated, including conventional classification queries, one-bit queries (Hu et al., 2020; Joshi et al., 2010) asking for yes or no answers, multi-class queries (Hwang et al., 2023) identifying all classes within a set of multiple instances, relative quires (Qian et al., 2013) asking for similarity of triplets, and correction queries (Kim et al., 2024) utilizing pseudo labels from the model. While these query methods require tailored loss functions, our candidate set query (CSQ) is cost-efficient and provides complete supervision, integrating seamlessly with existing loss functions. The approach closely related to CSO is the n-ary query (Bhattacharya & Chakraborty, 2019), which reduces the search space by asking for the correct class among top-n predictions of the model. However, the n-ary query uses a fixed number of top-n predictions for all data without considering individual sample difficulty. CSQ, on the other hand, adjusts the

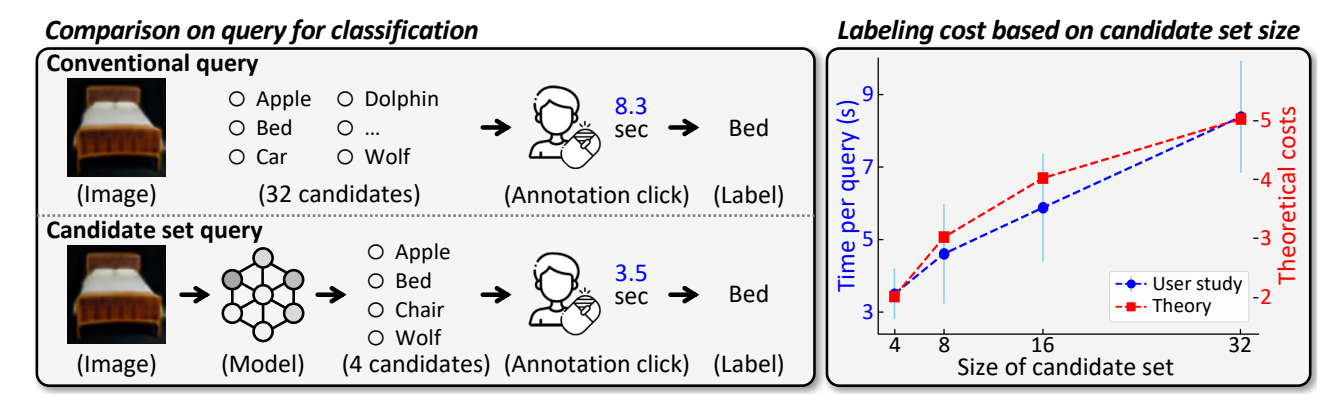


Figure 1: Conventional query versus CSQ. (*left*) While the conventional query presents all possible options to annotators, CSQ leverages the knowledge of the model to offer narrowed options that are likely to include the ground-truth label, thereby reducing the annotation time. (*right*) By conducting a user study on 40 participants, we demonstrate that the labeling cost increases logarithmically to the candidate set size, which closely aligns with the information-theoretic cost suggested by Hu et al. (2020) with a correlation coefficient of 0.97. Note that as the labeling cost increases per sample, the overall labeling cost increases significantly when multiplied by the total number of labeled samples. Further details of the user study are provided in Sec. 4.2 and Appendix A.

candidate set size based on sample difficulty and model performance using conformal prediction. Through rigorous comparisons, we demonstrate that CSQ achieves a superior model performance at the same cost compared to the previous query designs.

Conformal prediction (CP). CP enables us to quantify uncertainty in predictions with an associated confidence level (Shafer & Vovk, 2008). Recent advances in CP empower classifiers to generate predictive sets that include the true label with a probability chosen by the user (Angelopoulos et al., 2020; 2023). In the field of AL, nonconformity measurements from CP are employed in the acquisition function to select informative samples (Matiz & Barner, 2020). In contrast, we utilize CP not only to develop a cost-efficient acquisition function but also to design an efficient candidate set query reducing the labeling cost.

### 3 Proposed Method

We consider general classification tasks such that for input  $\mathbf{x}$  and a categorical variable  $y \in \mathcal{Y} = \{1, 2, \dots, L\}$ , a model parameterized by  $\boldsymbol{\theta}$  predicts the class of the input as  $\arg\max_{y \in \mathcal{Y}} P_{\boldsymbol{\theta}}(y|\mathbf{x})$ . We study an active learning (AL) scenario conducted over R rounds. In each round r, a budget of B samples is actively selected from the unlabeled data pool  $\mathcal{X}$  using an acquisition function. This actively selected set  $\mathcal{A}_r$  is then labeled by an annotator to form the labeled dataset  $\mathcal{D}_r$  with labeling cost  $C_r$ , and is used to update the model. Let  $\boldsymbol{\theta}_r$  denote the model trained on the accumulated labeled data up to round r,  $\bigcup_{i=0}^r \mathcal{D}_i$ . Our goal is to maximize the performance of  $\boldsymbol{\theta}_r$ , while minimizing the accumulated cost  $\bigcup_{i=0}^r C_i$ . The key aspect of the proposed

## Algorithm 1 Active learning with candidate set query

**Require:** The number of AL rounds R, per-round budget B, unlabeled data pool  $\mathcal{X}$ , Initial labeled dataset  $\mathcal{D}_0$ .

- 1: Train the initial model  $\theta_0$  on  $\mathcal{D}_0$ .
- 2: **for** r = 1, 2, ..., R **do**
- 3: Select the top B samples  $A_r \subset \mathcal{X}$  with highest acquisition scores  $g_{\text{cost}}(\mathbf{x})$ .  $\triangleright$  Sec. 3.3
- 4: Construct cost-efficient candidate set  $\hat{Y}(\mathbf{x})$  for each  $\mathbf{x} \in \mathcal{A}_r$ .  $\triangleright$  Sec. 3.2
- Query annotator for label y of x ∈ A<sub>r</sub> using candidate set Ŷ(x) to form D<sub>r</sub>.
- 6: Get model  $\theta_r$  trained on  $\bigcup_{i=0}^r \mathcal{D}_i$ .
- 7: end for
- 8: **Return** Final model  $\theta_R$ .

method is the candidate set query (CSQ), which reduces  $C_r$  by narrowing the set of candidate classes presented to annotators. For simplicity, we omit the round index r from  $\theta_r$  in the remainder of this section.

In the following, we first introduce CSQ and discuss its efficiency in labeling cost (Sec. 3.1). Then, we present a method to construct a candidate set based on the prediction uncertainty of a trained model for a given sample (Sec. 3.2). Lastly, we introduce an acquisition function designed to consider cost efficiency as well as information gain (Sec. 3.3). The overall pipeline of the CSQ framework is summarized in Algorithm 1.

### 3.1 Candidate set query

CSQ for an instance  $\mathbf{x}$  is associated with a (non-empty) candidate set  $\hat{Y}(\mathbf{x}) \subseteq \mathcal{Y}$  such that  $1 \leq |\hat{Y}(\mathbf{x})| \leq L$ . CSQ first asks the annotator to choose the ground-truth class in

 $\hat{Y}(\mathbf{x})$  (if exists) or to verify the absence of the ground-truth label in  $\hat{Y}(\mathbf{x})$ , *i.e.*, the annotator is first asked to pick an option out of (k+1) choices, where  $k=|\hat{Y}(\mathbf{x})|$ . Only if the absence of the ground-truth class in the candidate set is verified, the annotator is further asked to select the ground-truth class from the remaining ones  $\mathcal{Y}\setminus\hat{Y}(\mathbf{x})$ . To analyze the cost of CSQ, following the information-theoretic cost model (Hu et al., 2020) and our empirical study in Table. 1, we assume that the cost of choosing an option out of k many candidates is  $\log_2 k$ . Then, the labeling cost  $\Gamma(\hat{Y}(\mathbf{x}),y)$  of CSQ for input  $\mathbf{x}$ , ground-truth label y, and candidate set  $\hat{Y}(\mathbf{x})$  can be obtained as:

$$\Gamma(\hat{Y}(\mathbf{x}), y) = \begin{cases} \log_2(k+1) & \text{if } y \in \hat{Y}(\mathbf{x}) \\ \log_2(k+1) + \log_2(L-k) & \text{otherwise} \end{cases}.$$

The conventional query in AL is a special case of CSQ where  $\hat{Y}(\mathbf{x}) = \mathcal{Y}$ , and it is inefficient since the annotator must search through the entire set of size L with a cost of  $\log_2 L$ . The following theorem reveals the condition under which the expected cost of CSQ offers an improvement over that of the conventional query.

**Theorem 3.1.** Assume the information-theoretic cost model (Hu et al., 2020) of selecting one out of L possible options to be  $\log_2 L$ . Let  $L \geq 2$  be the number of classes,  $k = |\hat{Y}(\mathbf{x})|$ , and  $\alpha$  be the probability that the candidate set  $\hat{Y}(\mathbf{x})$  does not include the ground-truth class of instance  $\mathbf{x}$ . For the expected cost of conventional query  $C_{\text{con}}$  and that of candidate set query  $C_{\text{csq}}$ , if

$$\frac{\log_2(k+1)}{\log_2 L} < 1 - \alpha , \qquad (2)$$

then  $C_{\rm csq}(L, \mathbf{x}, \alpha) < C_{\rm con}(L, \mathbf{x})$ .

*Proof.* Recalling the definition of  $\alpha$ , we have  $C_{\rm csq}(L,{\bf x},\alpha)=(1-\alpha)\log_2(k+1)+\alpha\{\log_2(k+1)+\log_2(L-k)\}$  from Eq. (1). As L-k< L, the cost ratio of  $C_{\rm csq}(L,{\bf x},\alpha)$  to  $C_{\rm con}(L,{\bf x})$  for instance  ${\bf x}$  is induced as:

$$\frac{C_{\text{csq}}(L, \mathbf{x}, \alpha)}{C_{\text{con}}(L, \mathbf{x})} = \frac{\log_2(k+1) + \alpha \log_2(L-k)}{\log_2 L} 
< \frac{\log_2(k+1)}{\log_2 L} + \alpha.$$
(3)

Although we adopt the cost model from Hu et al. (2020), Theorem 3.1 holds for any cost model that increases monotonically with the number of options.

**Remark 3.2.** If we constrain all candidate set sizes k to be fixed, then  $1 - \alpha$  corresponds to the top-k accuracy  $p_k$  of the model. Therefore, when  $p_k \geq \log_L(k+1)$ , CSQ

consistently offers an improvement over the conventional query. For example, in datasets such as CIFAR-10 (L=10), CIFAR-100 (L=100), and ImageNet (L=1000), if the model has a top-1 accuracy (i.e., k=1) of at least 30.1%, 15.1%, and 10.0% respectively, then CSQ always provides an improvement.

The above proof and remark demonstrate that under moderate conditions, CSQ is more efficient than the conventional query. As described in Eq. (3), the cost of CSQ decreases as both  $\alpha$  and k become smaller. However, since k and  $\alpha$  are inversely related, balancing the trade-off between  $\alpha$  and k is essential to fully leverage CSQ. Also, fixing candidate set sizes as in Remark 3.2 is suboptimal because it does not consider the uncertainty of individual samples. In the following section, we introduce our candidate set construction method, which both reflects the uncertainty of each sample and automatically balances the trade-off between  $\alpha$  and k.

#### 3.2 Construction of cost-efficient candidate set

As shown in Eq. (1) and Theorem 3.1, a candidate set needs to be both small and accurate in covering the ground-truth class. To do so, we propose using conformal prediction (Romano et al., 2020) to get a reliable and cost-optimized prediction set using the trained model  $\theta$  of the previous round.

Calibration set collection. Conformal prediction requires a labeled set for calibration that has not been used during the model training phase; this set must follow the same distribution as the target data for prediction (Vovk et al., 1999; Angelopoulos et al., 2023). To achieve this, we randomly select  $n_{\rm cal}$  samples from the actively selected data  $\mathcal{A}_r$  and annotate them within the given budget to form  $\mathcal{D}_{\rm cal} = \{(\mathbf{x}_i, y_i)\}_{i=1}^{n_{\rm cal}}$ . The calibration set  $\mathcal{D}_{\rm cal}$  is used for conformal prediction and candidate set optimization, which will be explained in the following sections. Note that  $\mathcal{D}_{\rm cal}$  also contributes to model training after candidate set construction.

**Conformal prediction.** Using  $\boldsymbol{\theta}$  from the previous round and calibration set  $\mathcal{D}_{\text{cal}}$  randomly sampled from  $\mathcal{A}_r$ , we obtain a collection of conformal scores  $\mathbf{s} := \{s_i\}_{i \in [n_{\text{cal}}]}$ , where  $s_i := 1 - P_{\boldsymbol{\theta}}(y_i \mid \mathbf{x}_i)$  for  $(\mathbf{x}_i, y_i) \in \mathcal{D}_{\text{cal}}$ . Then, we obtain the  $(1 - \alpha)$  empirical quantile  $\hat{Q}(\alpha)$  of  $\mathbf{s}$ , indicating that at least  $100 \times (1 - \alpha)\%$  of the scores in  $\mathbf{s}$  are smaller than  $\hat{Q}(\alpha)$ . This quantile  $\hat{Q}(\alpha)$  is given as,

$$\hat{Q}(\alpha) := \min_{s \in \mathbf{s}} \left\{ s : \frac{1}{n_{\text{cal}}} \sum_{s' \in \mathbf{s}} \left( \mathbb{1}[s' \le s] \right) \ge 1 - \alpha \right\} , (4)$$

where  $\alpha \in (0,1)$  is an error rate hyperparameter, and  $\mathbb{1}[\cdot]$  is an indicator function. Then, we define the candidate set for unlabeled data  $\mathbf{x}$  as follows:

$$\hat{Y}_{\theta}(\mathbf{x}, \alpha) := \{ y : P_{\theta}(y|\mathbf{x}) \ge 1 - \hat{Q}(\alpha), \ y \in \mathcal{Y} \}$$
. (5)

Previous study (Vovk et al., 1999; Angelopoulos et al., 2023) proved that the candidate set includes the correct label with the probability not less than  $1 - \alpha$ , which is,

$$P(y \in \hat{Y}_{\theta}(\mathbf{x}, \alpha)) \ge 1 - \alpha$$
 (6)

This ensures the inclusion of the ground-truth classes even under model overconfidence, while adaptively reflecting uncertainties throughout the AL process. More detailed procedure of conformal prediction is in Appendix C.

Cost-optimized error rate selection. Although conformal prediction aims at adjusting candidate set  $\hat{Y}_{\theta}(\mathbf{x}, \alpha)$  to fit the condition of  $\alpha$  as in Eq. (6), it does not take into account the size k of the candidate set. The efficiency of CSQ improves as both  $\alpha$  and the candidate set size k decrease, as shown in Eq. (3). Since  $\alpha$  and k are inversely related, finding an optimal hyperparameter  $\alpha$  to reduce the labeling cost is not straightforward. Hence, we optimize  $\alpha$  to minimize labeling cost for the calibration set  $\mathcal{D}_{\text{cal}}$  for further improvement of CSQ efficiency. To be specific,  $\alpha$  is optimized by

$$\alpha^* := \underset{\alpha \in (0,1)}{\operatorname{arg \, min}} \sum_{(\mathbf{x}, y) \in \mathcal{D}_{\operatorname{cal}}} \Gamma(\hat{Y}_{\boldsymbol{\theta}}(\mathbf{x}, \alpha), y) , \qquad (7)$$

where  $\Gamma(\mathbf{x}, y, \hat{Y}_{\theta}(\mathbf{x}, \alpha))$  is the labeling cost in Eq. (1). By optimizing  $\alpha$  in this way, we utilize conformal prediction to construct candidate sets in a more cost-efficient manner, as the error rate is tailored to minimize the expected labeling cost for each round. Notably, if we define the corner case  $\hat{Y}_{\theta}(\mathbf{x},0) = \mathcal{Y}$ , CSQ includes the conventional query at  $\alpha = 0$  within the search space for  $\alpha^*$ . This makes CSQ is at least as efficient as, and in general more efficient than, the conventional query.

Note that to construct the candidate set query, the calibration set  $\mathcal{D}_{cal}$  is required to calculate  $(1-\alpha^*)$  quantile in Eq. (4). Thus, when getting annotations of  $\mathcal{D}_{cal}$  in the calibration set collection step, candidate set query of the current round cannot be applied. To avoid this circular dependency, the quantile from the previous round is used when labeling  $\mathcal{D}_{cal}$ .

## 3.3 Cost-efficient acquisition function

Since the labeling cost of each sample varies in CSQ, we propose to consider the cost for active sampling. We implement an acquisition function that evaluates samples based on the ratio of the estimated information gain to the estimated labeling cost. The information gain is quantified using established acquisition scores from prior research like entropy and SAAL (Kim et al., 2023), though our approach can integrate any acquisition scoring function. Given a conventional acquisition score  $g_{\text{score}}(\mathbf{x})$ , the proposed costefficient acquisition function  $g_{\text{cost}}$  is given as,

$$g_{\text{cost}}(\mathbf{x}) := \frac{(1 + g_{\text{score}}(\mathbf{x}))^d}{\log_2(k+1) + \alpha^* \log_2(L-k)},$$
 (8)

where d is a hyperparameter adjusting the influence of  $g_{\text{score}}(\mathbf{x})$  and  $\alpha^*$  is the optimized error rate hyperparameter obtained by Eq. (7). The denominator is an expected cost derived from our cost model (Eq. (1)), considering two cases: the correct label is included or excluded from the candidate set, which is  $(1-\alpha^*)\log_2(k+1)+\alpha^*\{\log_2(k+1)+\log_2(L-k)\}$ . This expected cost assumes the candidate set to include the ground-truth class with a probability of  $1-\alpha^*$ , which is supported by the coverage guarantee in Eq. (6).

## 4 Experiments

### 4.1 Experimental setup

**Datasets.** We use three image classification datasets: CIFAR-10 (Krizhevsky et al., 2009), CIFAR-100 (Krizhevsky et al., 2009), and ImageNet64x64 (Chrabaszcz et al., 2017). CIFAR-10 comprises 50K training and 10K validation images across 10 classes. CIFAR-100 contains the same number of images as CIFAR-10, but is associated with 100 classes. ImageNet64x64 is a downsampled version of ImageNet (Deng et al., 2009a) with a resolution of  $64 \times 64$ , which consists of 1.2M training and 50K validation images with 1000 classes. Following previous studies, we evaluate a model using the validation split of each dataset.

Implementation details. For CIFAR-10 and CIFAR-100, we adopt ResNet-18 (He et al., 2016) as a classification model. We train it for 200 epochs using AdamW (Loshchilov & Hutter, 2019) optimizer with an initial learning rate of 1e-3, decreasing by a factor of 0.2 at epochs 60, 120, and 160. We apply a weight decay of 5e-4and a data augmentation consists of random crop, random horizontal flip, and random rotation. For ImageNet64x64, we adopt WRN-36-5 (Zagoruyko, 2016), and train it for 30 epochs using AdamW optimizer with an initial learning rate of 8e-3. We apply a learning rate warm-up for 10 epochs from 2e-3. After the warm-up, we decay the learning rate by a factor of 0.2 every 10 epochs. We adopt random horizontal flip and random translation as data augmentation. For all the datasets, we use Mix-up (Zhang et al., 2018), where a mixing ratio is sampled from Beta(1, 1). We set the size of the calibration dataset  $n_{cal}$  to 500 for CIFAR-10 and CIFAR-100, and 5K for ImageNet64x64. For CIFAR-10 and CIFAR-100, d in Eq. (8) is set to 0.3 for all samplings. For ImageNet64x64, d is set to 1.2. The analysis of the impact of d and the dataset-wise guidelines for determining d are provided in Appendix H.

Active learning protocol. For CIFAR-10, we conduct 10 AL rounds of consecutive data sampling and model updates, while for CIFAR-100, we perform 9 AL rounds. In both cases, the per-round budget is 6K images. For Ima-

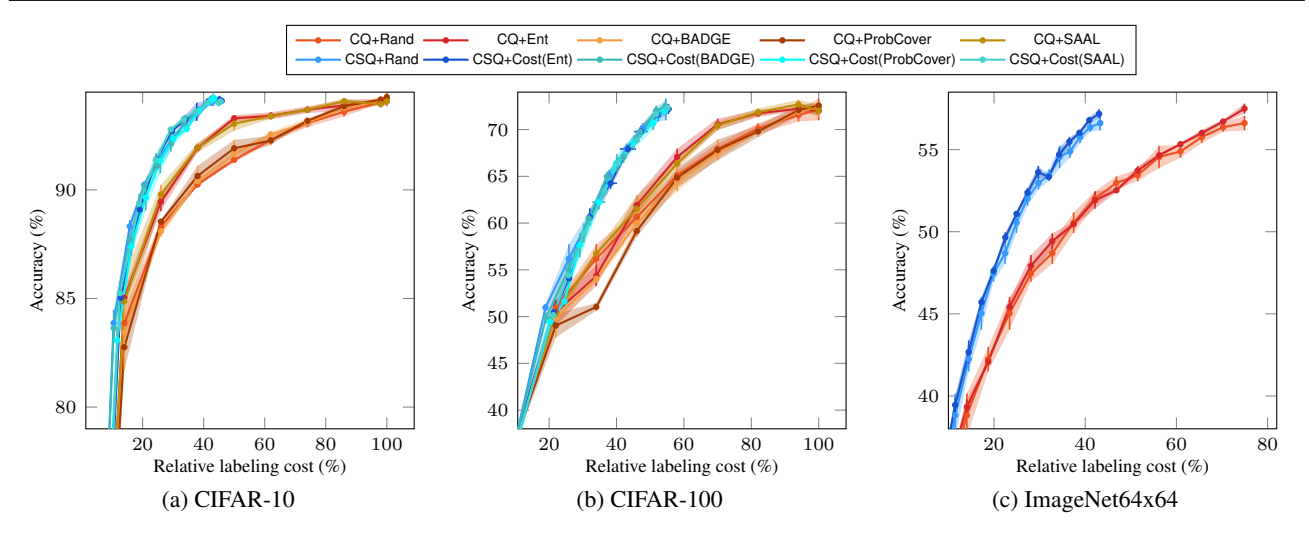


Figure 2: Accuracy (%) versus relative labeling cost (%) for conventional query (CQ) and the proposed candidate set query (CSQ) with different acquisition functions. CSQ approaches (blue lines) consistently outperform the CQ baselines (red lines) by a significant margin across various cost budgets, acquisition functions, and datasets. For ImageNet64x64, we report results of computationally tractable methods only.

geNet64x64, we conduct 16 AL rounds with a per-round budget of 60K images. The detailed budget configuration for the three datasets is shown in Table 4. In the initial round, we randomly sample 1K images for CIFAR-10, 5K images for CIFAR-100, and 60K images for ImageNet64x64. In each round, the model is evaluated based on two factors: its accuracy (%) on the validation set, and the accumulated annotation cost required to train it. The annotation cost is defined as a relative labeling cost (%) compared to the cost of labeling the entire training set using the conventional query, given by  $N \log_2 L$ , where N is the size of the entire training set, and L is the number of classes. We conduct all experiments with three independent trials with different random seeds and report the mean and standard deviation to ensure reproducibility.

Baseline methods. We compare our candidate set query (CSQ) with the conventional query (CQ) in combination with various sampling strategies. To be specific, we employ random (Rand), entropy (Ent), BADGE (Ash et al., 2020), ProbCover (Yehuda et al., 2022), and SAAL (Kim et al., 2023) as the sampling strategies. Cost(·) indicates the proposed cost-efficient sampling (Eq. (8)) using conventional acquisition scores; *e.g.*, Cost(SAAL) is the one combined with SAAL. We denote the combination of the query and sampling method with '+', *e.g.*, CSQ+Rand is a candidate set query with random sampling.

## 4.2 Experimental results

Candidate set query vs. Conventional query. In Figure 2, we compare the performance of the candidate set query (CSQ) with the conventional query (CQ) on CIFAR-

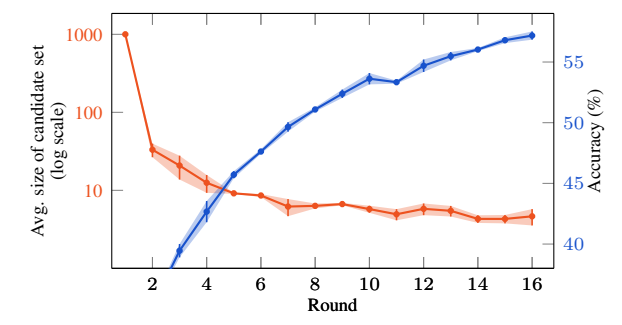
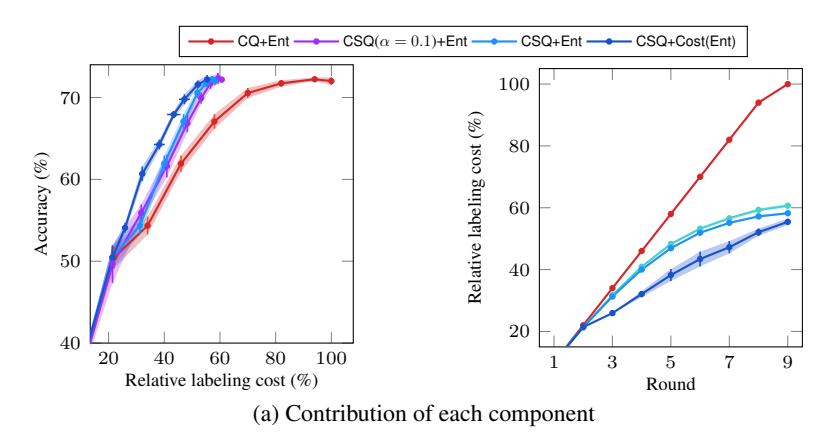


Figure 3: Average size of the candidate set and accuracy (%) of our method with Cost(Ent) sampling on ImageNet64x64. Our candidate set design adapts to the increasing accuracy of the model over AL rounds, reducing the size of the candidate set as the model improves, thereby enhancing efficiency of the labeling process.

Table 1: The results of the user study showing the annotation time (second) and accuracy (%) for the same images with varying size of class options (candidate set). This result demonstrates that a small candidate set improves both labeling efficiency and accuracy. The results also align closely with theoretical costs, as shown in Figure 1(right).

Set size	4	8	16	32
Time (s) Acc. (%)	$\begin{array}{ c c c c c c c c c c c c c c c c c c c$	$91.5_{\pm 27.3} \\ 98.5_{\pm 3.2}$	$116.9_{\pm 29.6} \\ 99.5_{\pm 1.5}$	$166.9_{\pm 30.8} \\ 95.5_{\pm 5.2}$

10, CIFAR-100, and ImageNet64x64 with different acquisition functions. CSQ approaches consistently outperform the CQ approaches across various acquisition functions and



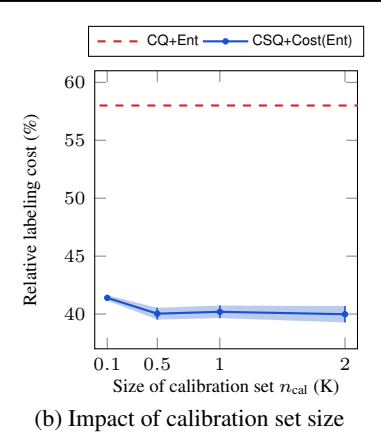


Figure 4: (a) Contribution of each component of our method, measured by accuracy (%) versus relative labeling cost (%) (left), and relative labeling cost (%) versus AL rounds (right) on CIFAR-100. The results compare the full method (CSQ+Cost(Ent)), the method without acquisition function in Eq. (8) (CSQ+Ent), without  $\alpha$  optimization in Eq. (7), where  $\alpha$  is fixed to 0.1 (CSQ( $\alpha=0.1$ )+Ent), and without CSQ (CQ+Ent). All components of our method lead to steady performance improvement over varying rounds. (b) Relative labeling cost (%) at the fifth round with varying calibration set sizes  $n_{\rm cal}$  in Eq. (4) on CIFAR-100. The dashed line indicates the relative labeling cost (%) of CQ+Ent. Our method shows consistent performance with varying calibration set sizes.

datasets, demonstrating the general effectiveness of our method. Notably, CSQ reduces the labeling cost of CQ by 43%, 54%, and 42% on CIFAR-10, CIFAR-100, and ImageNet64x64, respectively. This is promising as it shows that the same volume of labeled data can be obtained at roughly half the cost, without introducing any label noise or sample bias. Notably, the performance gain of CSQ increases as the model improves, as it is tailored to the improved model. In the appendix, we also present experiments on a text classification task (Figure 13) showing the generalization ability of the proposed method to the natural language domain. Additionally, we provide the zoomed version of Figure 2 in Figure 16 and Figure 17.

**Progressive reduction in candidate set size.** The effectiveness of CSQ stems from its ability to reduce labeling costs through smaller candidate sets. To verify this, Figure 3 shows the average size of the candidate sets and accuracy (%) of our method with varying AL rounds on ImageNet64x64. After the first round, CSQ achieves a sufficiently small candidate set size and continues to reduce it as accuracy improves. More results on CIFAR-10 and CIFAR-100 are shown in Figure 8.

Empirical validation for our cost model. We conduct a user study with 40 annotators who label samples using candidate sets of various sizes; see Appendix A for more details. The results in Table 1 suggest that reducing candidate sets improves both labeling efficiency and accuracy. They also align closely with the theoretical cost (Hu et al., 2020), as shown in Figure 1(right).

#### 4.3 Ablation studies

Contribution of each component. Figure 4a demonstrates the contribution of each component in our method across varying AL rounds: candidate set query (Eq. (5)), cost optimization of  $\alpha$  (Eq. (7)), and the proposed acquisition function (Eq. (8)). The results show consistent performance improvements from each component in every round. The performance gap between CQ+Ent and CSQ( $\alpha=0.1$ )+Ent verifies the efficacy of proposed CSQ framework, which provides the largest improvement. The gap between CSQ( $\alpha=0.1$ )+Ent and CSQ+Ent shows the impact of  $\alpha$  optimization, offering modest but steady gains across rounds. Finally, the gap between CSQ+Ent and CSQ+Cost(Ent) shows the effectiveness of our acquisition function, particularly from 4 to 6 rounds.

Impact of calibration set size. In Figure 4b, we evaluate the relative labeling cost (%) at the fifth round with varying calibration set sizes  $n_{\rm cal}$  in Eq. (4) to assess its impact on the performance on CIFAR-100. As shown in Figure 4b, our method shows consistent performance, varying by less than 2%p as the calibration set size changes from 0.1K to 2K, and significantly outperforms the baseline.

Ablation study on candidate set design. Figure 5 illustrates the effectiveness of using conformal prediction (Conformal ( $\alpha=0.1$ )) for candidate set construction on CIFAR-100, compared to baselines: Conventional (using all classes), Top1 (top-1 prediction), Top10 (top-10 predictions), and Oracle (smallest top-k set always containing the ground truth). Note that Oracle represents an unattainable upper bound requiring knowledge of the ground truth. Top1

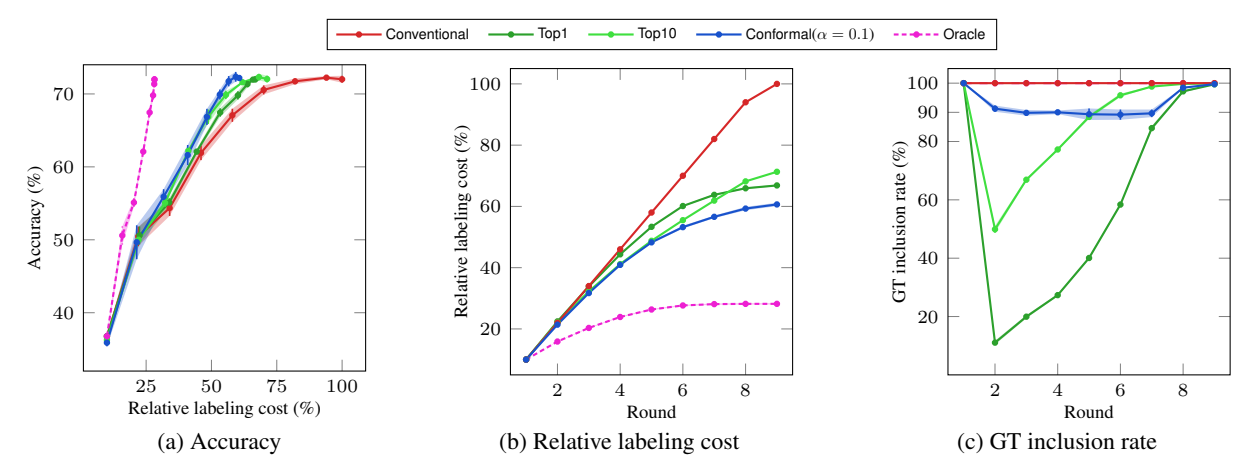


Figure 5: Impact of the candidate set design evaluated on CIFAR-100 using conventional query with all classes (Conventional), top-1 prediction from model (Top1), top-10 prediction from model (Top10), our method with conformal prediction with fixed  $\alpha=0.1$  (Conformal( $\alpha=0.1$ )), and the smallest top-k prediction sets always including ground-truth class (Oracle). For comparison, the same entropy sampling is used to keep the accuracy at each round constant, focusing solely on the labeling cost and isolating the effect of the candidate set design. (a) Our method constantly outperforms the baselines in accuracy (%) relative to labeling cost (%). (b) Our design achieves a greater reduction in labeling cost compared to the baselines. (c) Our candidate set effectively includes the ground-truth class in over 90% of cases (=  $1-\alpha$ ), even when model accuracy is low.

and Top10 are variants of the n-ary query (Bhattacharya & Chakraborty, 2019) baseline. For consistency, we fixed  $\alpha = 0.1$  in Eq. (5). Figures 5a and 5b show that conformal prediction consistently reduces labeling cost compared to the baselines. While Top10 is effective in the early rounds and Top1 becomes more efficient as the model improves, our method adapts throughout and outperforms all baselines in every round. Figure 5c demonstrates that with  $\alpha = 0.1$ , our method includes the ground-truth class in over 90% of cases, aligning with Eq. (6), while the top-k baselines show lower inclusion rates, especially in early and middle rounds. This demonstrates that conformal prediction effectively adjusts candidate set sizes based on sample uncertainty, ensuring ground-truth inclusion and improving labeling efficiency. Examples of the candidate sets on ImageNet64x64 are presented in Figure 9.

Impact of cost-efficient acquisition function. In Table 2, we investigate the impact of the proposed cost-efficient sampling (Sec. 3.3) on CIFAR-100, in terms of accuracy per relative labeling cost. Our cost-efficient sampling strategy consistently improves the cost-effectiveness across various conventional acquisition functions.

### 4.4 Additional experiments

In the appendix, we provide additional results verifying the impact of cost-optimized error rate selection in Eq. (7) (Figure 10), generalization ability to language domain (Figure 13), and robustness to label noise (Figure 14) and class imbalance (Figure 15).

Table 2: Effectiveness of the proposed cost-efficient sampling (Cost(·)) with CSQ evaluated on CIFAR-100, measured by accuracy per cost.

Sampling	3 rd round	6 th round	9 th round
Ent	1.74	1.36	1.24
Cost(Ent)	2.09	1.56	1.30
ProbCover	1.72	1.47	1.30
Cost(ProbCover)	2.10	1.66	1.32
SAAL	1.83	1.37	1.25
Cost(SAAL)	2.12	1.64	1.31

### 5 Conclusion

We have introduced candidate set query, an active learning framework that efficiently reduces the labeling cost by narrowing down the candidate set likely to include the ground-truth class. We also have proposed a novel acquisition function that balances model performance and labeling cost by taking expected candidate set sizes into account. Experiments on CIFAR-10, CIFAR-100, and ImageNet64x64 confirm the effectiveness of our framework.

**Limitations and future work.** One limitation is that the proposed acquisition function lacks theoretical guarantee for label complexity (Dasgupta, 2011; Hanneke et al., 2014) at this point. Establishing a theoretical understanding to quantify the cost required to achieve a target performance remains an interesting direction for future work.

## **6** Impact Statements

This research contributes to effectively reducing annotation costs in data collection for real-world applications. To the best of our knowledge, we do not identify any significant negative societal implications that need to be addressed.

### References

- Angelopoulos, A. N., Bates, S., Jordan, M., and Malik, J. Uncertainty sets for image classifiers using conformal prediction. In *Proc. International Conference on Machine Learning (ICML)*, 2020.
- Angelopoulos, A. N., Bates, S., et al. Conformal prediction: A gentle introduction. *Foundations and Trends® in Machine Learning*, 16(4):494–591, 2023.
- Asghar, N., Poupart, P., Jiang, X., and Li, H. Deep active learning for dialogue generation. In *Proceedings of the 6th Joint Conference on Lexical and Computational Semantics* (\*SEM), 2017.
- Ash, J. T., Zhang, C., Krishnamurthy, A., Langford, J., and Agarwal, A. Deep batch active learning by diverse, uncertain gradient lower bounds. In *Proc. International Conference on Learning Representations (ICLR)*, 2020.
- Bhattacharya, A. R. and Chakraborty, S. Active learning with n-ary queries for image recognition. In *Proc. IEEE/CVF Winter Conference on Applications of Computer Vision (WACV)*, 2019.
- Cho, S. J., Kim, G., Lee, J., Shin, J., and Yoo, C. D. Querying easily flip-flopped samples for deep active learning. In *The Twelfth International Conference on Learning Representations, ICLR* 2024, 2024.
- Chrabaszcz, P., Loshchilov, I., and Hutter, F. A down-sampled variant of imagenet as an alternative to the cifar datasets. *arXiv preprint arXiv:1707.08819*, 2017.
- Cortes, C. Support-vector networks. *Machine Learning*, 1995.
- Cui, Y., Jia, M., Lin, T.-Y., Song, Y., and Belongie, S. Class-balanced loss based on effective number of samples. In *Proceedings of the IEEE/CVF conference* on computer vision and pattern recognition, pp. 9268– 9277, 2019.
- Dasgupta, S. Two faces of active learning. *Theoretical computer science*, 412(19):1767–1781, 2011.
- Deng, J., Dong, W., Socher, R., Li, L.-J., Li, K., and Fei-Fei, L. Imagenet: A large-scale hierarchical image database. In 2009 IEEE Conference on Computer Vision and Pattern Recognition, pp. 248–255, 2009a. doi: 10.1109/CVPR.2009.5206848.

- Deng, J., Dong, W., Socher, R., Li, L.-J., Li, K., and Fei-Fei, L. ImageNet: a large-scale hierarchical image database. In *Proc. IEEE/CVF Conference on Computer Vision and Pattern Recognition (CVPR)*, 2009b.
- Du, P., Zhao, S., Chen, H., Chai, S., Chen, H., and Li, C. Contrastive coding for active learning under class distribution mismatch. In *Proc. IEEE/CVF International Conference on Computer Vision (ICCV)*, pp. 8927–8936, 2021.
- Fang, A., Ilharco, G., Wortsman, M., Wan, Y., Shankar, V., Dave, A., and Schmidt, L. Data determines distributional robustness in contrastive language image pretraining (clip). In *Proc. International Conference on Machine Learning (ICML)*, pp. 6216–6234. PMLR, 2022.
- Frénay, B. and Verleysen, M. Classification in the presence of label noise: a survey. *IEEE transactions on neural networks and learning systems*, 25(5):845–869, 2013.
- Fuchsgruber, D., Wollschläger, T., Charpentier, B., Oroz, A., and Günnemann, S. Uncertainty for active learning on graphs. In *Forty-first International Conference on Machine Learning*, 2024.
- Hacohen, G. and Weinshall, D. How to select which active learning strategy is best suited for your specific problem and budget. In Oh, A., Naumann, T., Globerson, A., Saenko, K., Hardt, M., and Levine, S. (eds.), *Advances in Neural Information Processing Systems*, volume 36, pp. 13395–13407. Curran Associates, Inc., 2023a.
- Hacohen, G. and Weinshall, D. How to select which active learning strategy is best suited for your specific problem and budget. *Advances in Neural Information Processing Systems*, 36, 2023b.
- Hacohen, G., Dekel, A., and Weinshall, D. Active learning on a budget: Opposite strategies suit high and low budgets. In *International Conference on Machine Learning*, pp. 8175–8195. PMLR, 2022.
- Hanneke, S. et al. Theory of disagreement-based active learning. *Foundations and Trends® in Machine Learning*, 7(2-3):131–309, 2014.
- He, K., Zhang, X., Ren, S., and Sun, J. Deep residual learning for image recognition. In *Proceedings of the IEEE conference on computer vision and pattern recognition*, pp. 770–778, 2016.
- He, T., Jin, X., Ding, G., Yi, L., and Yan, C. Towards better uncertainty sampling: Active learning with multiple views for deep convolutional neural network. In *IEEE International Conference on Multimedia and Expo (ICME)*, 2019.

- Hestness, J., Narang, S., Ardalani, N., Diamos, G., Jun, H., Kianinejad, H., Patwary, M. M. A., Yang, Y., and Zhou, Y. Deep learning scaling is predictable, empirically. arXiv preprint arXiv:1712.00409, 2017.
- Hu, H., Xie, L., Du, Z., Hong, R., and Tian, Q. One-bit supervision for image classification. *Proc. Neural In*formation Processing Systems (NeurIPS), 33:501–511, 2020.
- Hu, J., Shen, L., and Sun, G. Squeeze-and-excitation networks. In Proc. IEEE/CVF Conference on Computer Vision and Pattern Recognition (CVPR), 2018.
- Hwang, S., Lee, S., Kim, S., Ok, J., and Kwak, S. Combating label distribution shift for active domain adaptation. In *Proc. European Conference on Computer Vision (ECCV)*, pp. 549–566. Springer, 2022.
- Hwang, S., Lee, S., Kim, H., Oh, M., Ok, J., and Kwak, S. Active learning for semantic segmentation with multiclass label query. *Advances in Neural Information Pro*cessing Systems, 36, 2023.
- Joshi, A. J., Porikli, F., and Papanikolopoulos, N. Breaking the interactive bottleneck in multi-class classification with active selection and binary feedback. In *Proc. IEEE/CVF Conference on Computer Vision and Pattern Recognition (CVPR)*, 2010.
- Kim, H., Hwang, S., Kwak, S., and Ok, J. Active label correction for semantic segmentation with foundation models. In *Proc. International Conference on Machine Learning (ICML)*, 2024.
- Kim, Y.-Y., Cho, Y., Jang, J., Na, B., Kim, Y., Song, K., Kang, W., and Moon, I.-C. Saal: sharpness-aware active learning. In *Proc. International Conference on Machine Learning (ICML)*, 2023.
- Kirillov, A., Mintun, E., Ravi, N., Mao, H., Rolland, C., Gustafson, L., Xiao, T., Whitehead, S., Berg, A. C., Lo, W.-Y., et al. Segment anything. In *Proc. IEEE International Conference on Computer Vision (ICCV)*, pp. 4015–4026, 2023.
- Kirsch, A., Van Amersfoort, J., and Gal, Y. Batchbald: Efficient and diverse batch acquisition for deep bayesian active learning. *Proc. Neural Information Processing Systems (NeurIPS)*, 32, 2019.
- Kothawade, S., Beck, N., Killamsetty, K., and Iyer, R. Similar: Submodular information measures based active learning in realistic scenarios. *Proc. Neural Information Processing Systems (NeurIPS)*, 34:18685–18697, 2021.
- Krishnamurthy, A., Agarwal, A., Huang, T.-K., Daumé III, H., and Langford, J. Active learning for cost-sensitive

- classification. *Journal of Machine Learning Research*, 20(65):1–50, 2019.
- Krizhevsky, A., Hinton, G., et al. Learning multiple layers of features from tiny images. 2009.
- Lewis, D. D. Reuters-21578 text categorization test collection, 1997. URL http://www.daviddlewis.com/resources/testcollections/reuters21578/.
- Liu, Y., Li, Z., Zhou, C., Jiang, Y., Sun, J., Wang, M., and He, X. Generative adversarial active learning for unsupervised outlier detection. *IEEE Transactions on Knowledge and Data Engineering*, 32(8):1517–1528, 2019.
- Loshchilov, I. and Hutter, F. Decoupled weight decay regularization. In *Proc. International Conference on Learn*ing Representations (ICLR), 2019.
- Matiz, S. and Barner, K. E. Conformal prediction based active learning by linear regression optimization. *Neurocomputing*, 388:157–169, 2020.
- Ning, K.-P., Zhao, X., Li, Y., and Huang, S.-J. Active learning for open-set annotation. In *Proc. IEEE/CVF Conference on Computer Vision and Pattern Recognition (CVPR)*, pp. 41–49, 2022.
- OpenAI. Gpt-4 technical report. *arXiv preprint arXiv*:2303.08774, 2023.
- Ostapuk, N., Yang, J., and Cudré-Mauroux, P. Activelink: deep active learning for link prediction in knowledge graphs. In *The World Wide Web Conference (WWW)*, 2019.
- Park, D., Shin, Y., Bang, J., Lee, Y., Song, H., and Lee, J.-G. Meta-query-net: Resolving purity-informativeness dilemma in open-set active learning. *Proc. Neural Information Processing Systems (NeurIPS)*, 35:31416–31429, 2022.
- Qian, B., Wang, X., Wang, F., Li, H., Ye, J., and Davidson, I. Active learning from relative queries. In *Proc. International Joint Conference on Artificial Intelligence (IJCAI)*, 2013.
- Qu, C., Zhang, T., Qiao, H., Tang, Y., Yuille, A. L., Zhou, Z., et al. Abdomenatlas-8k: Annotating 8,000 ct volumes for multi-organ segmentation in three weeks. Advances in Neural Information Processing Systems, 36, 2024.
- Radford, A., Kim, J. W., Hallacy, C., Ramesh, A., Goh, G., Agarwal, S., Sastry, G., Askell, A., Mishkin, P., Clark, J., et al. Learning transferable visual models from natural language supervision. In *Proc. International Conference*

- on Machine Learning (ICML), pp. 8748–8763. PMLR, 2021.
- Romano, Y., Sesia, M., and Candes, E. Classification with valid and adaptive coverage. *Proc. Neural Information Processing Systems (NeurIPS)*, 33:3581–3591, 2020.
- Sener, O. and Savarese, S. Active learning for convolutional neural networks: A core-set approach. In *Proc. International Conference on Learning Representations* (ICLR), 2018.
- Settles, B. Active learning literature survey. Computer Sciences Technical Report 1648, University of Wisconsin–Madison, 2009.
- Shafer, G. and Vovk, V. A tutorial on conformal prediction. *Journal of Machine Learning Research*, 9(3), 2008.
- Sinha, S., Ebrahimi, S., and Darrell, T. Variational adversarial active learning. In *Proc. IEEE/CVF International Conference on Computer Vision (ICCV)*, 2019.
- Tran, T., Do, T.-T., Reid, I., and Carneiro, G. Bayesian generative active deep learning. In *International conference on machine learning*, pp. 6295–6304. PMLR, 2019.
- Vovk, V., Gammerman, A., and Saunders, C. Machine-learning applications of algorithmic randomness. In *Proc. International Conference on Machine Learning (ICML)*, ICML '99, pp. 444–453, San Francisco, CA, USA, 1999. Morgan Kaufmann Publishers Inc. ISBN 1558606122.
- Wang, D., Zhang, J., Du, B., Xu, M., Liu, L., Tao, D., and Zhang, L. Samrs: Scaling-up remote sensing segmentation dataset with segment anything model. *Advances in Neural Information Processing Systems*, 36, 2024.
- Wang, Z. and Ye, J. Querying discriminative and representative samples for batch mode active learning. *ACM Transactions on Knowledge Discovery from Data* (*TKDD*), 2015.
- Wang, Z., Du, B., Tu, W., Zhang, L., and Tao, D. Incorporating distribution matching into uncertainty for multiple kernel active learning. *IEEE Transactions on Knowledge and Data Engineering (TKDE)*, 2019.
- Yang, Y., Zhang, Y., Song, X., and Xu, Y. Not all out-of-distribution data are harmful to open-set active learning. *Proc. Neural Information Processing Systems* (*NeurIPS*), 36, 2024.
- Yehuda, O., Dekel, A., Hacohen, G., and Weinshall, D. Active learning through a covering lens. Advances in Neural Information Processing Systems, 35:22354–22367, 2022.

- Zagoruyko, S. Wide residual networks. *arXiv preprint arXiv:1605.07146*, 2016.
- Zhai, X., Kolesnikov, A., Houlsby, N., and Beyer, L. Scaling vision transformers. In *Proc. IEEE Conference on Computer Vision and Pattern Recognition (CVPR)*, pp. 12104–12113, 2022.
- Zhang, H., Cisse, M., Dauphin, Y. N., and Lopez-Paz, D. mixup: Beyond empirical risk minimization. In *International Conference on Learning Representations*, 2018.

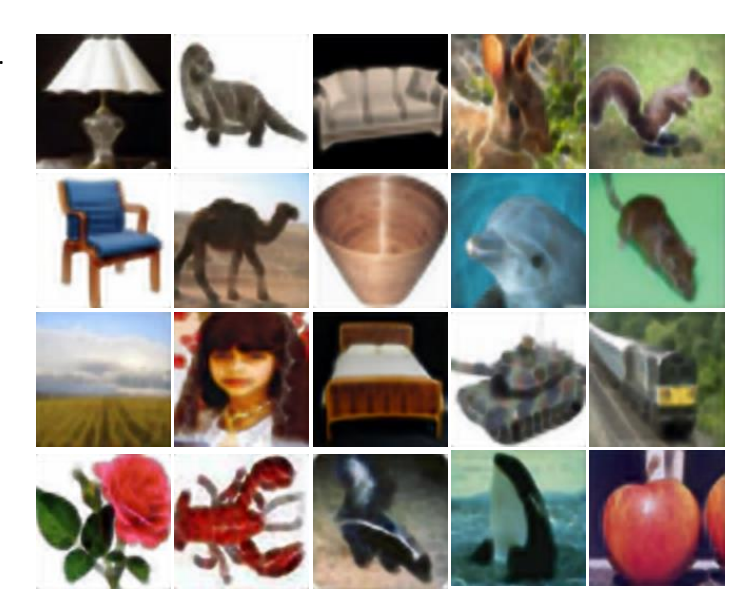
# **Enhancing Cost Efficiency in Active Learning with Candidate Set Query**

# —Appendix—

# A Details of user study

Q. Select the class that corresponds to the image.





(a) Questionnaire with four candidates (k = 4)

(b) Example queries in CIFAR-100

Figure 6: Questionnaire and examples used in the user study. (a) Each question contains an instruction, an image, and a set of candidates. In this case, the candidate set size is 4. (b) We utilize 20 images in CIFAR-100, each with a resolution of 128 x 128 pixels.

We conduct a user study to examine how the size of a candidate set, k in Sec. 3.1, affects the annotation time in practice. Figure 6 presents examples of the questionnaire and all images used in our user study. To facilitate easy comparison with the theoretical costs (Hu et al., 2018), we set the candidate set sizes to 4, 8, 16, and 32. To be specific about Figure 6, we use CIFAR-100 images resized to  $128 \times 128$  using super resolution to enhance visibility for annotators. We first randomly select 20 classes in CIFAR-100 and choose one image per class to organize the questionnaires. For small-sized candidate sets, we ensure the inclusion of the ground truth by randomly trimming around it when generating the candidate sets.

We divide 44 annotators into four groups of 11 for each candidate set size to perform labeling tasks. To account for potential outliers, we exclude the results of the annotators whose time taken deviates the most from the average time in each group. Table 3 shows that as the candidate set size increases, the time per query increases and the accuracy decreases. In addition, on the right side of Table 3, the comparison between the experimental costs and theoretical costs reveals a significant correlation of 0.97.

Table 3: User study for different sizes of candidate set query.

k	Total time (s)	Time per query (s)	Accuracy (%)	Experimental	Theoretical
4	<b>69.4</b> <sub>±13.8</sub>	<b>3.47</b> <sub>±0.69</sub>	$100.0_{\pm 0.0}$	2.0	2
8	$91.5_{\pm 27.3}$	$5.20_{\pm 1.36}$	$98.5_{\pm 3.2}$	2.6	3
16	$116.9_{\pm 29.6}$	$6.94_{\pm 1.48}$	$99.5_{\pm 1.5}$	3.4	4
32	$166.9_{\pm 30.8}$	$8.35_{\pm 1.54}$	$95.5_{\pm 5.2}$	4.8	5

<sup>&</sup>lt;sup>1</sup>https://www.kaggle.com/datasets/joaopauloschuler/cifar100-128x128-resized-via-cai-super-resolution

## **B** Implementation details and configuration

Table 4 presents the configuration of our main experiments for each dataset. In all experiments, we fixed the per-round budget, which limits the number of annotated instances per active learning (AL) round. Given this budget constraint, we compute the labeling cost for each AL round to assess labeling efficiency. The batch size for CIFAR-10 and CIFAR-100 was determined to be 128, while that for ImageNet64x64 is set to 128. We normalized the input image to ensure the stability of the training. We trained our classification model on CIFAR-10 and CIFAR-100 using NVIDIA RTX 3090 and on ImageNet64x64 using 4 NVIDIA A100 GPUs in parallel. The training requires about 5 GPU hours for CIFAR-10 and CIFAR-100, and about 1.5 GPU days for ImageNet64x64.

Dataset	L	${\rm log}_2 L$	Size	Cost of full label	# of rounds	Per-round budget
CIFAR-10	10	3.322	50K	166.1K	10	6K
CIFAR-100	100	6.644	50K	332.2K	9	6K
ImageNet64x64	1000	9.966	1.2M	12.7M	16	60K

Table 4: Detailed dataset and budget configuration for the proposed scenario.

Code. This part demonstrates the reproducibility of our work by providing comprehensive details on the source code release. We have made available the entire framework, which includes the data sampling methods, evaluation procedures, and the overall training pipeline. Our aim is to ensure that other researchers can easily replicate and build upon our results. To get started with running the code, please refer to the script.sh and readme.md files. readme.md contains the instructions to comprehend and execute our experiments seamlessly, and script.sh includes some example commands. To understand our proposed method better, you can examine the Python script al/strategy\_dtopk.py. This file includes the implementation details of our active learning strategies, particularly *candidate set query* design. Furthermore, our code can run on CIFAR-100 <sup>2</sup>, and ImageNet64x64 <sup>3</sup>, which are available online. Note that you can modify the running configuration such as dataset, sampling method, and budget through command-line arguments.

## C Additional clarification on candidate set construction

The detailed procedure of computing  $\hat{Q}(\alpha)$  in Eq. (4). We begin with computing the collection of conformal scores s for the calibration dataset  $\mathcal{D}_{cal}$ . For each data point  $(\mathbf{x}_i, y_i) \in \mathcal{D}_{cal}$ , the conformal score is defined as:

$$s_i := 1 - P_{\theta}(y_i \mid \mathbf{x}_i), \quad \text{for } i = 1, 2, \dots, n_{\text{cal}},$$
 (9)

where  $n_{\text{cal}} = |\mathcal{D}_{\text{cal}}|$ . Using these scores, we define the empirical distribution function  $F_n(s)$ , which measures the proportion of scores less than or equal to a given value s. Formally,  $F_n(s)$  is expressed as:

$$F_n(s) = \frac{1}{n_{\text{cal}}} \sum_{i=1}^{n_{\text{cal}}} \mathbb{1}[s_i \le s] , \qquad (10)$$

where  $\mathbb{1}[\cdot]$  is an indicator function. The  $(1-\alpha)$  empirical quantile is then defined as the smallest score  $s_i$  such that the proportion of scores satisfying  $s_i \leq s$  is at least  $(1-\alpha)$ . Mathematically, this is given as  $\min_{i \in [n_{\text{cal}}]} \{F_n(s_i) \geq 1-\alpha\}$ , where  $[n_{\text{cal}}] = \{1, 2, \cdots, n_{\text{cal}}\}$ .

$$\hat{Q}(\alpha) := \min_{i \in [n_{\text{cal}}]} \{ F_n(s_i) \ge (1 - \alpha) \} . \tag{11}$$

Note that Eq. (11) is equivalent to Eq. (4).

## D Impact of proposed cost-efficient sampling across different sampling strategies

Figure 2 illustrates that combining CSQ with our cost-efficient sampling method results in a significant performance improvement. Additionally, Figure 4a examines how the cost-efficient sampling improves performance compared to using

https://www.cs.toronto.edu/~kriz/cifar.html

https://patrykchrabaszcz.github.io/Imagenet32/

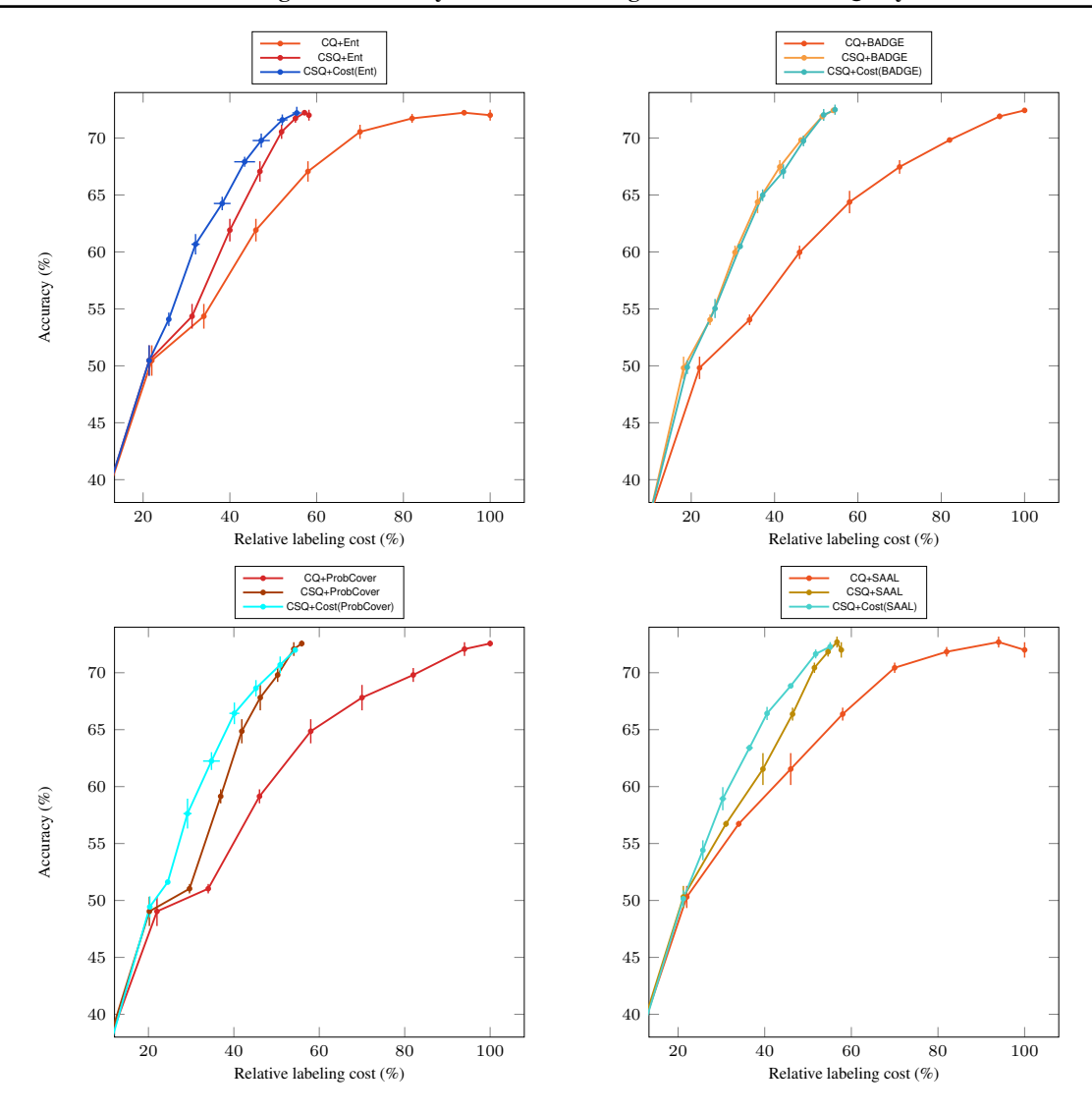


Figure 7: Comparison of different sampling methods and their cost-sampling variants on CIFAR-100. Each subplot shows a pair of corresponding methods.

CSQ alone. In this section, we compare different sampling strategies when combined with their cost-efficient variants. Notably, the performance of cost-efficient sampling improves substantially when paired with Ent, ProbCover, and SAAL. This demonstrates that our cost-efficient acquisition method (Eq. (8)) can be integrated with any sample-wise acquisition strategy, including but not limited to entropy-based sampling, ProbCover (Yehuda et al., 2022), and SAAL (Kim et al., 2023). However, BADGE (Ash et al., 2020) does not involve sample-wise acquisition and instead performs random sampling based on k-means++ initialization. This explains why CSQ+Cost(BADGE) does not outperform CSQ+BADGE. Nevertheless, this is not a major drawback, CSQ+BADGE itself without cost-efficient sampling still achieves significantly better performance compared to CQ+BADGE.

## E Change in candidate set size across rounds

In Figure 8, we show that the CSQ effectively reduces the candidate set size k throughout AL rounds on CIFAR-10, CIFAR-100, and ImageNet64x64 datasets. After the first round, CSQ achieves a sufficiently small candidate set size and continues to reduce it as accuracy improves, thereby enhancing labeling efficiency.

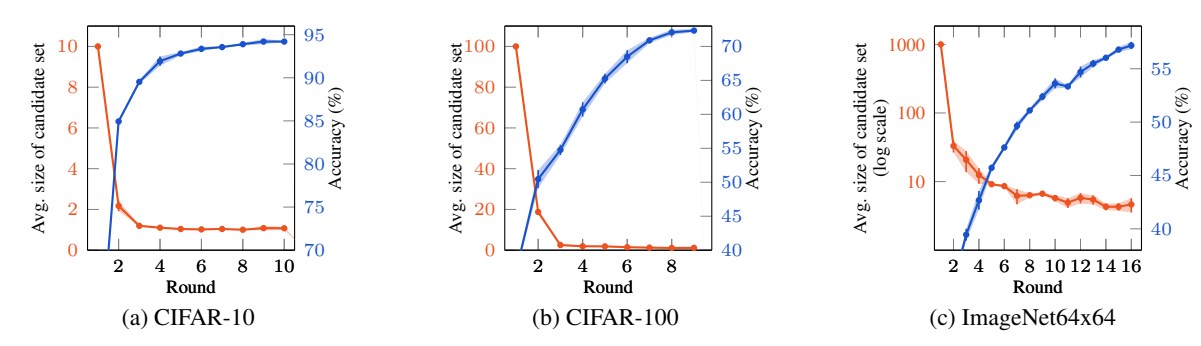


Figure 8: Average size of the candidate set and accuracy (%) of our method with cost-efficient entropy sampling in varying rounds on CIFAR-10, CIFAR-100, and ImageNet64x64. Our candidate set design adapts to the increasing accuracy of the model over successive AL rounds, reducing it as the model improves.



Figure 9: Examples of input images and their corresponding candidate sets constructed from our method in fifth round on ImageNet64x64. The ground-truth class is highlighted in red (best viewed in color).

# F Examples of constructed candidate sets

In Figure 9, we present example results showing input images and their corresponding candidate sets on ImageNet64x64. Thanks to the conformal prediction, the proposed method allows for flexible adjustment of the candidate set for each sample. For certain samples (Figure 9(left)), the candidate set is reduced to minimize labeling cost, while for uncertain samples (Figure 9(right)), the candidate set is expanded to include the true label.

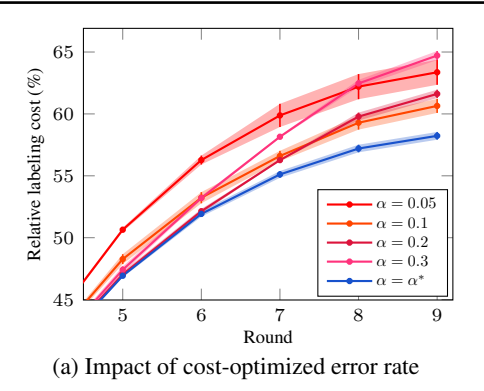
### **G** Impact of cost-optimized error rate selection

In Figure 10, we present the impact of cost-optimized error rate selection as in Eq. (7), evaluated on CIFAR-100 using entropy sampling, in terms of relative labeling cost (%). As shown in Figure 10a, the proposed optimization consistently reduces labeling cost across all rounds by selecting the optimal  $\alpha = \alpha^*$ . In Figure 10b, the pink triangle indicate how the most cost-effective  $\alpha$  changes with each active learning round, showing that labeling costs vary depending on the chosen  $\alpha$ . Our method enhances cost efficiency by selecting the  $\alpha^*$  (blue square) in each round through cost optimization.

## **H** Impact of hyperparameter d

Impact of informativeness-cost balancing hyperparameter d. The hyperparameter d in our acquisition function (Eq. (8)) balances the trade-off between labeling cost and the informativeness of a selected sample, requiring both factors to be considered. We provide a comprehensive analysis showing the trend of performance in accuracy with varying d values over AL rounds for CIFAR-10, CIFAR-100, and ImageNet64x64 in Figure 11. For CIFAR-10 (Figure 11a), both accuracy and labeling cost remain robust to the change of d, varying only 0.5%p in accuracy. For CIFAR-100 (Figure 11b), the overall performance is still insensitive yet slightly increasing as d decreases. For ImageNet64x64 (Figure 11c), on the other hand, the performance decreases as d increases. Regarding that a larger d prioritizes more uncertain samples, this result aligns with recent observations in AL that uncertainty-based selection performs better in scenarios with larger labeling budgets (Hacohen et al., 2022).

Guidelines for selecting proper hyperparameter d. We provide the following guidelines for setting d. For datasets with



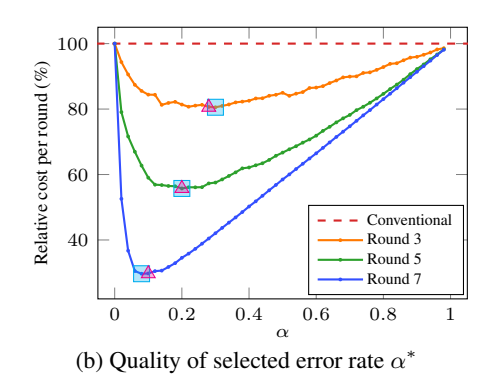


Figure 10: Impact of cost-optimized error rate selection as in Eq. (7), evaluated on CIFAR-100 with entropy sampling. (a) Relative labeling cost (%) versus AL rounds with different error rate  $\alpha$  and the  $\alpha^*$  selected by the proposed cost optimization (Eq. (7)). (b) Relative labeling cost per round (%) versus  $\alpha$  across varying AL rounds. Labeling cost is measured as the ratio compared to labeling all images in a single round using the conventional query. The pink triangle represents the true optimal  $\alpha$  minimizing the cost for sampled data, while the blue square represents the  $\alpha^*$  selected from Eq. (7). The red dashed line indicates the baseline cost from the conventional query.

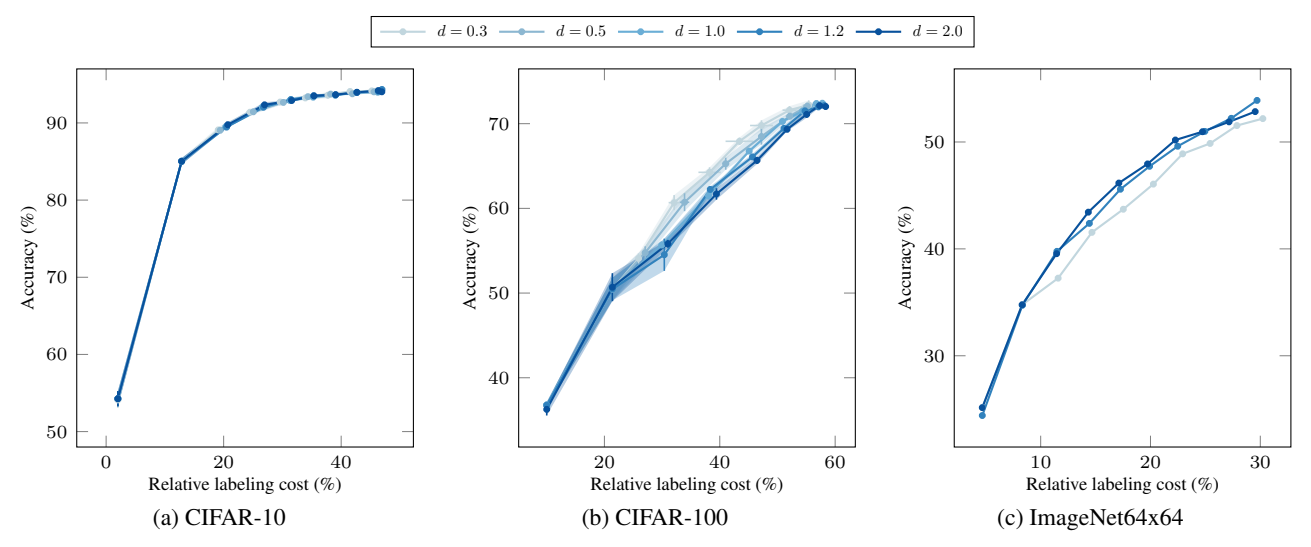


Figure 11: Accuracy (%) versus relative labeling cost (%) with varying hyperparameter d in Eq. (8) across AL rounds, evaluated on CIFAR-10, CIFAR-100 and ImageNet64x64 with CSQ+Cost(Ent). For our main experiments, we set d=0.3 for CIFAR-10 and CIFAR-100, and d=1.2 for ImageNet64x64.

fewer than 100 classes, d values between 0.3 and 1.0 may be effective, as they ensure robustness on simple datasets like CIFAR-10 and reduce labeling costs on more complex datasets like CIFAR-100. For larger datasets closer in scale to ImageNet, exploring  $d \ge 1.0$  can help further improve the model performance.

## I Discussion on handling outliers and anomalous datapoints

Dealing with out-of-distribution (OOD) data points showing high uncertainty scores has been a chronic issue in active learning and may affect the efficiency of candidate set query (CSQ). Recent open-set active learning approaches (Du et al., 2021; Kothawade et al., 2021; Ning et al., 2022; Park et al., 2022; Yang et al., 2024) tackle this by filtering out OOD samples during active sampling using an OOD classifier. Our CSQ framework integrates seamlessly with these methods, focusing on labeling in-distribution (ID) samples to prevent cost inefficiencies.

However, as OOD classifiers are not flawless, some OOD samples may still be selected. One advantage of our method is its ability to leverage the calibration set to capture information about such mixed OOD samples. This enables adjustments

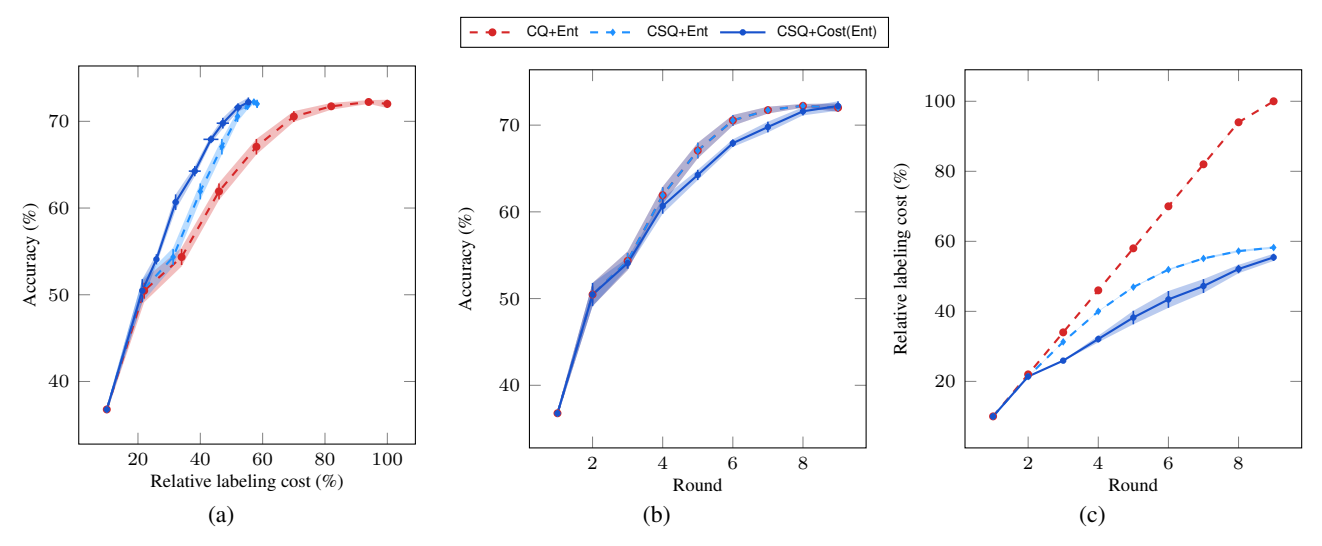


Figure 12: Comparison of candidate set query (CSQ) and conventional query (CQ) on CIFAR-100 with entropy sampling (Ent) and cost-efficient entropy sampling (Cost(Ent)) varying AL rounds. A fixed number of samples are selected at each AL round. (a) Accuracy (%) versus relative labeling cost (%) showing the accuracy per cost. (b) Accuracy (%) versus AL rounds showing the accuracy varies with the number of samples. Note that the lines of CQ+Ent and CSQ+Ent completely overlap, as they use the same sampling method. (c) Relative labeling cost (%) versus AL rounds.

such as increasing the OOD classifier threshold to exclude more OOD-like data or incorporating the OOD ratio into the alpha optimization process in Eq. (7). Optimizing the combination of OOD and ID classifier scores within the calibration set or designing better OOD-aware queries presents promising future research directions.

## J Compatibility between candidate set construction and uncertain samples

Figure 12 compares CSQ and conventional query (CQ) on CIFAR-100 with entropy-based sampling (Ent) and our acquisition function with entropy measure (Cost(Ent), Eq. (8)) across AL rounds, with a fixed number of samples per round.

Our acquisition function provides superior accuracy per cost. The comparison between CSQ+Cost(Ent) and CSQ+Ent demonstrates that the proposed acquisition function reduces labeling costs with only a marginal accuracy trade-off.

Candidate set query (CSQ) can reduce labeling costs even for uncertain samples. The comparison between CQ+Ent and CSQ+Ent demonstrates that CSQ effectively reduces labeling costs, even with uncertainty-based sampling methods like entropy sampling. This shows that CSQ can narrow down annotation options even for uncertain samples. Note that CSQ+Ent shows the same accuracy as CQ+Ent, since they used the same sampling method.

## K Experiments in language domain

**Dataset.** The R52 dataset (Lewis, 1997) is a subset of the Reuters-21578 (Lewis, 1997) news collection, specifically curated for text classification tasks. It comprises documents categorized into 52 distinct classes, with a total of 9,130 documents. The dataset is divided into 6,560 training documents and 2,570 testing documents. Each document is labeled with a single category, and the categories are selected to ensure that each has at least one document in both the training and testing sets. This structure makes the R52 dataset particularly suitable for evaluating text classification models.

**Implementation details.** We adopt an SVM model (Cortes, 1995) with sigmoid kernel for classification. We conduct 11 AL rounds of consecutive data sampling and model updates, where the per-round budget is 600. The hyperparameter d for our acquisition function is set as 1.2. In the initial round, we randomly sample 300 samples. In each round, the model is evaluated based on three factors: its accuracy (%) and Micro-F1 (%).

Figure 13 presents a comparison of candidate set query (CSQ) and conventional query (CQ) on the text classification dataset (R52) with random sampling (Rand), entropy sampling (Ent), and our acquisition function with entropy measure (Cost(Ent), Eq. (8)) across AL rounds. CSQ approaches consistently outperform the CQ baselines by a significant margin

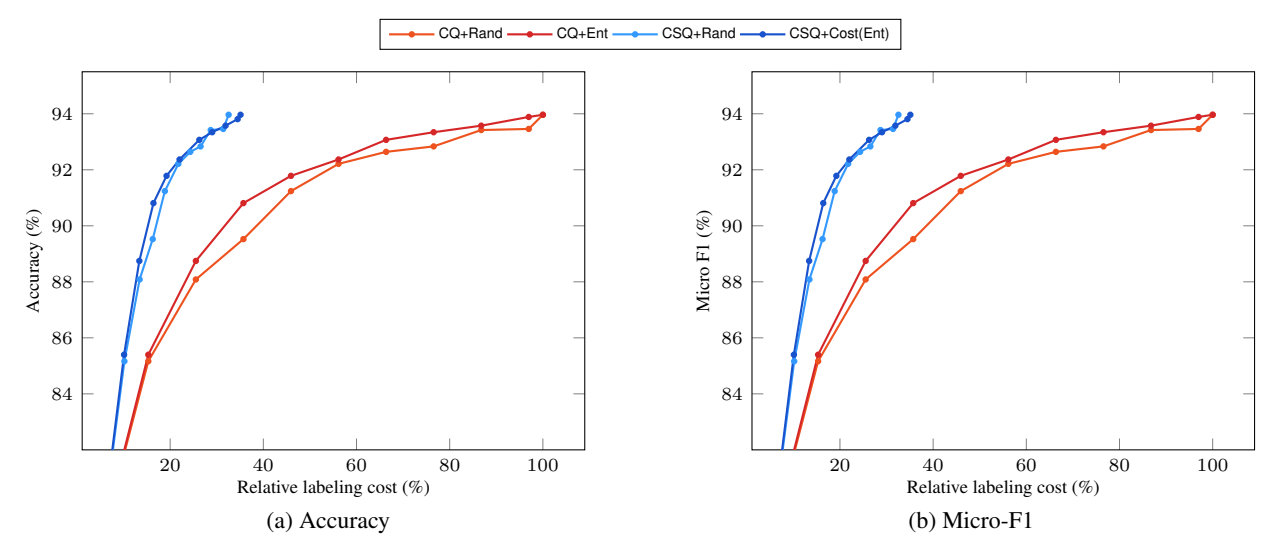


Figure 13: Comparison between conventional query (CQ) and candidate set query (CSQ) with random sampling (Rand), entropy sampling (Ent), and cost-efficient entropy sampling (Cost(Ent) on text classification task with R52 dataset. (a) Accuracy (%) versus relative labeling cost (%). (b) Micro-F1 (%) versus relative labeling cost (%). CSQ approaches (blue lines) consistently outperform the CQ baselines (red lines) by a significant margin across various budgets and acquisition functions.

across various budgets and acquisition functions. Especially at round 10, CSQ+Rand reduces labeling cost by 65.6%p compared to its conventional query baseline. The result demonstrates that the proposed CSQ framework generalizes to the text classification domain.

## L Experiments on real-world datasets

**Experiment on datasets containing label noise.** We evaluate the candidate set query (CSQ) framework on CIFAR-100 with noisy labels, simulating a scenario where human annotators misclassify images into random classes with a noise rate  $\epsilon$ . This is modeled using a uniform label noise (Frénay & Verleysen, 2013) with  $\epsilon$  set to 0.05 and 0.1. Note that this scenario is unfavorable for CSQ, as a misclassifying annotator would reject the actual true label even if the candidate set includes it. Figure 14 compares CSQ and conventional query (CQ) on CIFAR-100 with noisy labels using entropy sampling (Ent) and our acquisition function with entropy measure (Cost(Ent)) across 2, 6, and 9 rounds.

Despite the disadvantageous scenario, our method (CSQ+Cost(Ent)) reduces labeling cost compared to the baseline (CQ+Ent) across varying AL rounds and noise rates. At round 9, CSQ+Cost(Ent) achieves cost reductions of 33.4%p and 27.4%p at noise rates of 0.05 and 0.1, respectively. It also consistently outperforms the baseline in terms of accuracy per labeling cost, demonstrating the robustness of CSQ. Additionally, CSQ has the potential to reduce label noise, as narrowing the candidate set can lead to more precise annotations. Our user study (Table 1) shows that reducing candidate set size improves annotation accuracy, suggesting that CSQ can further enhance performance by reducing label noises.

**Experiment on datasets containing class imbalances.** Figure 15 compares candidate set query (CSQ) and conventional query (CQ) on CIFAR-100-LT (Cui et al., 2019), a class-imbalanced version of CIFAR-100, using entropy sampling (Ent), and our acquisition function with entropy measure (Cost(Ent)) across AL rounds. The experiments use imbalance ratios (*i.e.*, ratios between the largest and smallest class sizes) of 3, 6, and 10. Note that the maximum AL rounds vary with the imbalance ratio due to dataset size, with a maximum of 4 rounds for ratios of 3 and 6, and 6 rounds for a ratio of 10.

The result shows that our method (CSQ+Cost(Ent)) reduces labeling cost compared to the baselines (CQ+Ent) by significant margins across varying AL rounds and imbalance ratios. Specifically, at round 4, CSQ+Cost(Ent) achieves cost reductions of 31.1%p and 29.2%p at imbalance ratios of 6 and 10, respectively. In terms of accuracy per labeling cost, CSQ+Cost(Ent) consistently outperforms the baseline, demonstrating the robustness of the CSQ framework in class-imbalanced scenarios.

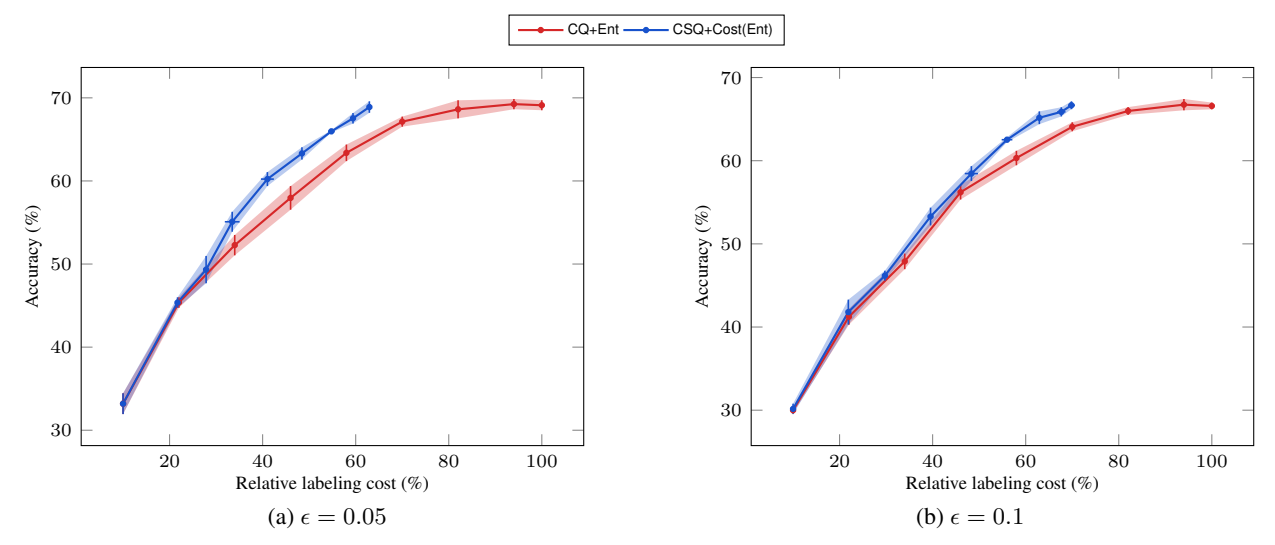


Figure 14: Comparison between conventional query (CQ) and candidate set query (CSQ) with entropy sampling (Ent) and the proposed acquisition function with entropy measure (Cost(Ent) on CIFAR-100 with label noise across AL rounds with varying noise level: (a) Noise rate of 0.05. (b) Noise rate of 0.1. The proposed CSQ+Cost(Ent) consistently outperforms CSQ+Ent across various AL rounds and noise rates.

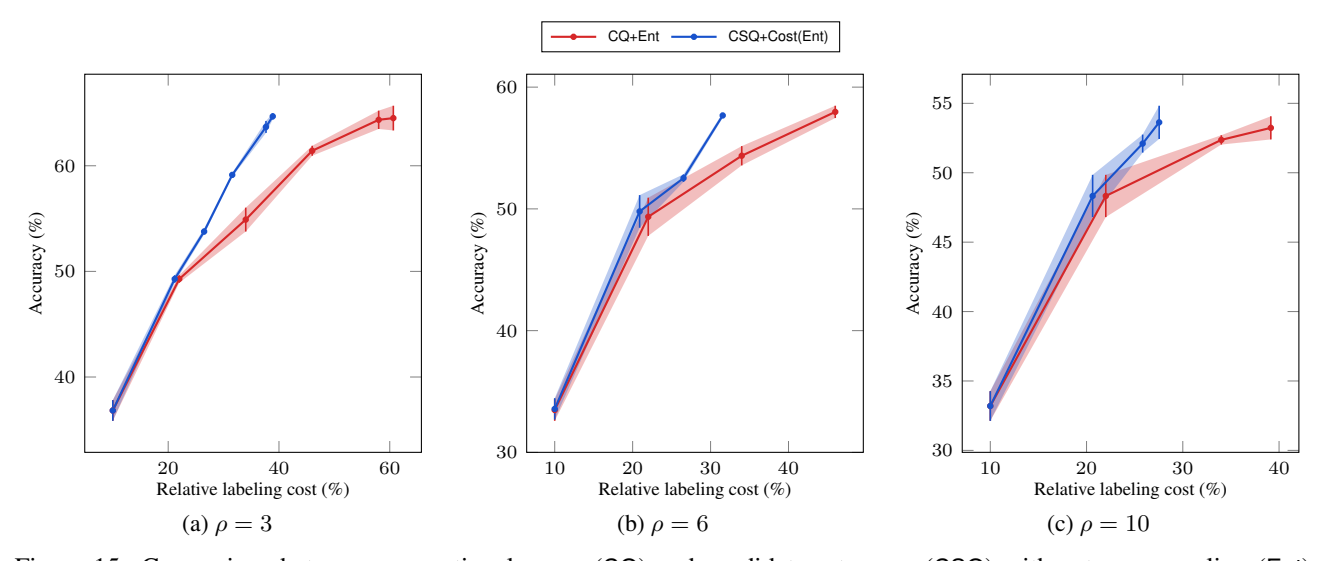


Figure 15: Comparison between conventional query (CQ) and candidate set query (CSQ) with entropy sampling (Ent) and the proposed acquisition function with entropy measure (Cost(Ent) on CIFAR-100-LT, a variant of CIFAR-100 with class imbalance, across AL rounds with varying imbalance level: (a) Imbalance ratio of 3. (b) Imbalance ratio of 6. (c) Imbalance ratio of 10. The proposed approach (CSQ+Cost(Ent)) consistently outperforms the baseline (CSQ+Ent) across various AL rounds and noise rates. Note that the maximum AL rounds vary with the imbalance ratio due to dataset size, with a maximum of 4 rounds for ratios of 3 and 6, and 6 rounds for a ratio of 10.

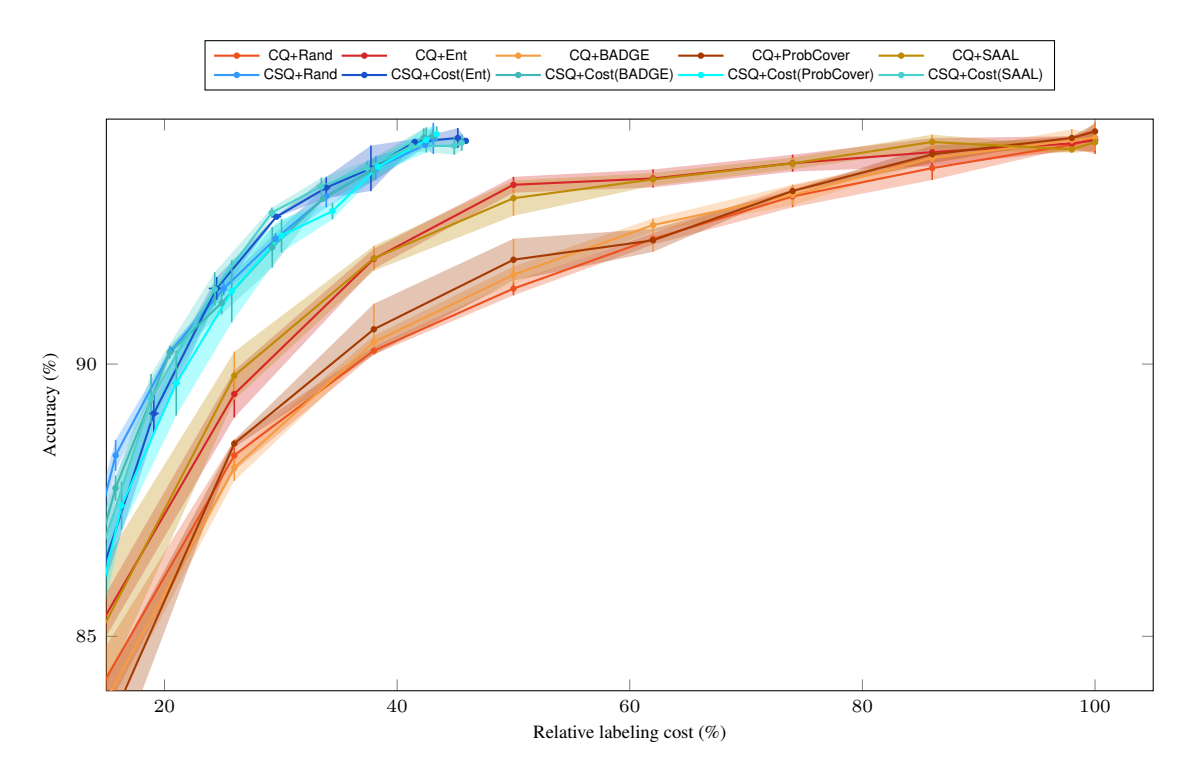


Figure 16: Accuracy (%) versus relative labeling cost (%) on CIFAR-10.

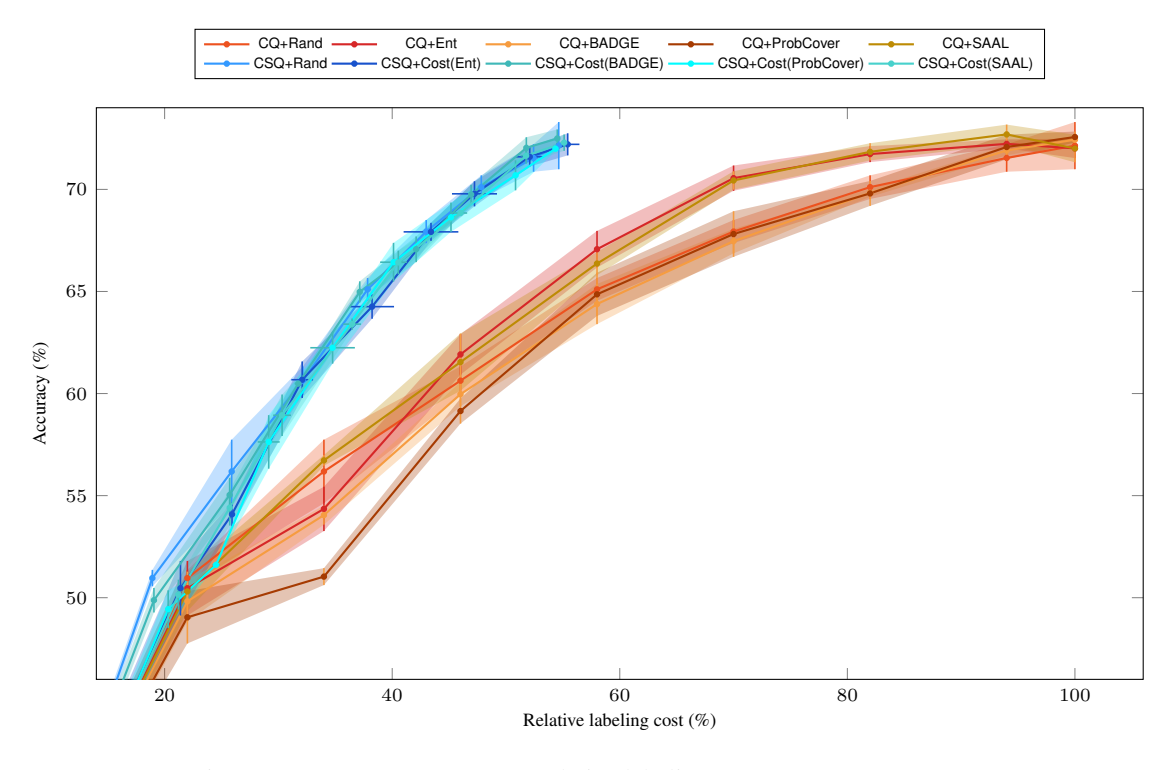


Figure 17: Accuracy (%) versus relative labeling cost (%) on CIFAR-100.